LETTER Communicated by Barbara Hammer

Sequential Triangle Strip Generator Based on Hopfield Networks

Jiří Šíma
sima@cs.cas.cz
Institute of Computer Science, Academy of Sciences of the Czech Republic, P.O. Box 5, 18207 Prague 8, Czech Republic

Radim Lněnička
r.lnenicka@centrum.cz
Institute of Information Theory and Automation, Academy of Sciences of the Czech Republic, Prague, Czech Republic

The important task of generating the minimum number of sequential triangle strips (tristrips) for a given triangulated surface model is motivated by applications in computer graphics. This hard combinatorial optimization problem is reduced to the minimum energy problem in Hopfield nets by a linear-size construction. In particular, the classes of equivalent optimal stripifications are mapped one to one to the minimum energy states reached by a Hopfield network during sequential computation starting at the zero initial state. Thus, the underlying Hopfield network powered by simulated annealing (i.e., Boltzmann machine), which is implemented in the program HTGEN, can be used for computing the semioptimal stripifications. Practical experiments confirm that one can obtain much better results using HTGEN than by a leading conventional stripification program FTSG (a reference stripification method not based on neural nets), although the running time of simulated annealing grows rapidly near the global optimum. Nevertheless, HTGEN exhibits empirical linear time complexity when the parameters of simulated annealing (i.e., the initial temperature and the stopping criterion) are fixed and thus provides the semioptimal offline solutions, even for huge models of hundreds of thousands of triangles, within a reasonable time.

1 Sequential Triangle Strips

Piecewise-linear surfaces defined by sets of triangles (triangulations) are widely used representations for geometric models. Computing a succinct encoding of a triangulated surface model represents an important problem in graphics and visualization. Current 3D graphics-rendering hardware often faces a memory bus bandwidth bottleneck in the processor-to-graphics pipeline. Apart from reducing the number of triangles that must

Neural Computation **21, 583–617** (2009)

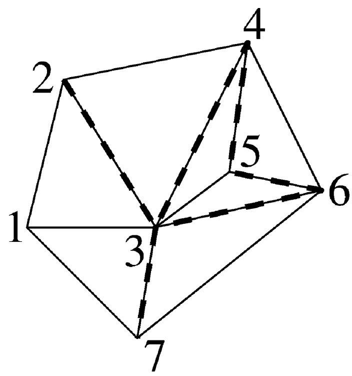

Figure 1: Tristrip (1,2,3,4,5,6,3,7,1).

be transmitted, it is also important to encode the triangulated surface efficiently. A common encoding scheme is based on sequential triangle strips, which avoid repeating the vertex coordinates of shared triangle edges. Triangle strips are supported by several graphics libraries (e.g., IGL, PHIGS, Inventor, OpenGL).

In particular, a sequential triangle strip (hereafter tristrip) of length $m-2$ is an ordered sequence of $m \geq 3$ vertices $\sigma = (v_1, \ldots, v_m)$, which encodes the set of $n(\sigma) = m-2$ different triangles $T_\sigma = \{\{v_p, v_{p+1}, v_{p+2}\} \mid 1 \leq p \leq m-2\}$ so that their shared edges follow alternating left and right turns, as indicated in Figure 1 by the dashed lines. Thus, a triangulation consisting of a single tristrip with n triangles allows transmitting only $n+2$ (rather than $3n$) vertices. In general, a triangulated surface model T with n triangles that is decomposed into k disjoint tristrips $\Sigma = \{\sigma_1, \ldots, \sigma_k\}$ requires only $n+2k$ vertices to be transmitted. A crucial problem is to decompose a triangulated surface model into the fewest tristrips. This stripification problem was proven to be NP-complete (Estkowski, Mitchell, & Xiang, 2002). A more detailed comparison of conventional stripification algorithms including relevant references has recently been presented by Vaněček and Kolingerová (2007).

In this letter, a new method of generating tristrips for a given triangulated surface model T with n triangles, which is based on a linear-time reduction to the minimum energy problem in a Hopfield network $\mathcal{H}_T$ with $O(n)$ units and $O(n)$ connections, is proposed. This approach has been inspired by a more complicated and incomplete reduction (e.g., sequential cycles were not excluded) introduced by Pospíšil and Zbořil (2004), which was supported only by experiments.

The letter is organized as follows. After a brief review of basic definitions concerning Hopfield nets in section 2, the main construction of Hopfield network $\mathcal{H}_T$ for a given triangulation T is described in section 3.

The correctness of this reduction is formally verified in section 4 by proving a one-to-one correspondence between the classes of equivalent optimal stripifications of T and the minimum energy states reached by $\mathcal{H}_T$ during sequential computation starting at the zero initial state (or $\mathcal{H}_T$ can be initialized arbitrarily if one asymmetric weight is introduced). This provides another NP-completeness proof for the minimum energy problem in Hopfield nets.

In addition, $\mathcal{H}_T$ combined with simulated annealing (i.e., Boltzmann machine) has been implemented in a program HTGEN (available online at http://www.cs.cas.cz/~sima/htgen-en.html). In section 5, HTGEN is compared to a leading stripification program FTSG (Xiang, Held, & Mitchell, 1999), which is considered to be a reference stripification method not based on neural nets. Practical experiments show that HTGEN can compute much better stripifications than FTSG, although the HTGEN running time grows rapidly when the global optimum is being approached. Furthermore, we study empirically how to choose the parameters of simulated annealing (i.e., the initial temperature and the stopping criterion) so that the correct stripification with a given number of tristrips is obtained in the shortest time. Moreover, the experiments show the average linear time complexity of HTGEN when the parameters of simulated annealing are fixed. Thus, one can use HTGEN for finding the semioptimal offline solutions even for huge models of hundreds of thousands of triangles within a reasonable time.

A preliminary version of this letter appeared as extended abstracts (Šíma, 2005a, 2005b) containing first practical experiments with HTGEN using grid models and a proof sketch, respectively.

2 The Minimum Energy Problem

Hopfield (1982) introduced an influential associative memory model that has since come to be widely known as the (symmetric) Hopfield network. The fundamental characteristic of this model is its well-constrained convergence behavior as compared to arbitrary asymmetric networks. Part of the appeal of Hopfield nets stems from their connection to the much-studied Ising spin glass model in statistical physics (Barahona, 1982) and their natural hardware implementations using electrical networks (Hopfield, 1984) or optical computers (Farhat, Psaltis, Prata, & Paek, 1985). Hopfield networks have also been applied to the fast approximate solution of combinatorial optimization problems (Cichocki & Unbehauen, 1993; Hopfield & Tank, 1985).

Formally, a Hopfield network is composed of s computational units or neurons, indexed as $N = \{1, \ldots, s\}$, that are connected into an undirected graph or architecture, in which each connection between unit i and j is labeled with an integer symmetric weight $w(i, j) = w(j, i)$. The absence of a connection within the architecture indicates a zero weight between the respective neurons, and vice versa. Hereafter we assume $w(j, j) = 0$ for every $j = 1, \ldots, s$. The sequential discrete dynamics of such a network is considered here, in which the evolution of the network state $\mathbf{y}^{(t)} = (y_1^{(t)}, \ldots, y_s^{(t)}) \in \{0, 1\}^s$ is determined for discrete time instants $t = 0, 1, 2, \ldots$ as follows. The initial state $\mathbf{y}^{(0)}$ may be chosen arbitrarily, for example, $\mathbf{y}^{(0)} = (0, \ldots, 0)$. At discrete time $t \geq 0$, the excitation of any neuron j is defined as

$$\xi_j^{(t)} = \sum_{i=1}^{s} w(i, j) y_i^{(t)} - h(j), \tag{2.1}$$

including an integer threshold $h(j)$ local to unit j. At the next instant $t+1$, one (e.g., randomly) selected neuron j computes its new output $y_j^{(t+1)} = H(\xi_j^{(t)})$ by applying the Heaviside activation function $H(\xi)$ defined to be 1 for $\xi \geq 0$ and 0 for $\xi < 0$, that is, j becomes active when $H(\xi_j^{(t)}) = 1$, while j will be passive otherwise. The remaining units do not change their states, that is, $y_i^{(t+1)} = y_i^{(t)}$ for $i \neq j$. In this way, the new network state $\mathbf{y}^{(t+1)}$ at time $t+1$ is determined.

In order to avoid long, constant intermediate computations when only units that effectively do not change their outputs are updated, a macroscopic time $\tau = 0, 1, 2, \ldots$ is introduced during which all the units in the network are updated. A computation of a Hopfield network converges or reaches a stable state $\mathbf{y}^{(\tau^*)}$ at macroscopic time $\tau^* \geq 0$ if $\mathbf{y}^{(\tau^*)} = \mathbf{y}^{(\tau^*+1)}$. The well-known fundamental property of a symmetric Hopfield network is that its dynamics is constrained by the energy function

$$E(\mathbf{y}) = -\frac{1}{2} \sum_{j=1}^{s} \sum_{i=1}^{s} w(i, j) y_i y_j + \sum_{j=1}^{s} h(j) y_j, \tag{2.2}$$

which is a bounded function defined on its state space whose value decreases along any nonconstant computation path (to be precise, it is assumed here without loss of generality that $\xi_j^{(t)} \neq 0$; Parberry, 1994). It follows from the existence of such a function that starting from any initial state, the network converges toward some stable state corresponding to a local minimum of E (Hopfield, 1982). Thus, the cost function of a hard combinatorial optimization problem can be encoded into the energy function of a Hopfield network, which is then minimized in the course of computation. Hence, the minimum energy problem of finding a network state with minimum energy is of special interest. Nevertheless, this problem is in general NP-complete (Barahona, 1982; see also the review by Šíma & Orponen, 2003, for related results).

A stochastic variant of the Hopfield model, the Boltzmann machine (Ackley, Hinton, & Sejnowski, 1985), is also considered in which a randomly selected unit j becomes active at time $t+1$ ($y_j^{(t+1)} = 1$), with probability $P(\xi_j^{(t)})$ computed by applying the probabilistic activation function $P : \Re \longrightarrow (0, 1)$ defined as

$$P(\xi) = \frac{1}{1 + e^{-2\xi/T^{(\tau)}}}, \tag{2.3}$$

where $T^{(\tau)} > 0$ is the so-called temperature at macroscopic time $\tau \geq 0$. This parameter is controlled by simulated annealing, for example,

$$T^{(\tau)} = \frac{T^{(0)}}{\log_2(1 + \tau)}, \tag{2.4}$$

for $\tau > 0$ and sufficiently high initial temperature $T^{(0)}$. Simulated annealing is a powerful heuristic method for avoiding the local minima in combinatorial optimization.

3 The Reduction

3.1 Sequential Cycles. For the purpose of our reduction, the following definitions are introduced. Let T be a set of n triangles that represents a triangulated two-manifold surface model of genus 0 (possibly with boundaries) in which each edge is incident to at most two triangles. Moreover, choose and fix one of the two possible orientations of this surface. An edge is said to be internal if it is shared by exactly two triangles; otherwise it is a boundary edge. Denote by I and B the sets of internal and boundary edges, respectively, in the triangulation T. We will say that a tristrip σ traverses an internal edge e by the left turn or counterclockwise if the next edge e' to be traversed occurs on the left (with respect to the surface orientation) when one enters the triangle given by e, e' by crossing the edge e orthogonally. We speak about the right turns or the clockwise traversal in analogous manner. Thus, for instance, the tristrip depicted in Figure 1 traverses the edge $\{3, 4\}$ counterclockwise, by the left turn, while the edge $\{6, 3\}$ is traversed by this strip clockwise, by the right turn, with respect to the natural orientation (from the air).

Furthermore, a sequential cycle is a "cycled tristrip," that is, an ordered sequence of vertices $c = (v_1, \ldots, v_m)$ such that $v_{m-1} = v_1$ and $v_m = v_2$ where $m \geq 4$ is even, which encodes the set of $m - 2$ different triangles $T_c = \{\{v_p, v_{p+1}, v_{p+2}\} \mid 1 \leq p \leq m - 2\}$. Also denote by I_c and B_c the sets of internal and boundary edges of sequential cycle c, respectively, that is, $I_c = \{\{v_p, v_{p+1}\} \mid 1 \leq p \leq m - 2\}$ and $B_c = \{\{v_p, v_{p+2}\} \mid 1 \leq p \leq m - 2\}$. An example of the sequential cycle is depicted in Figure 2 where its internal and

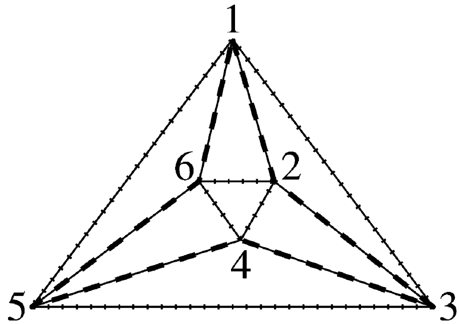

Figure 2: Sequential cycle (1,2,3,4,5,6,1,2).

boundary edges are indicated by the dashed and dotted lines, respectively. Let C be the set of all sequential cycles in T. This set can easily be generated in linear time as follows.

Observe first that for the fixed orientation of triangulated surface, a tristrip can traverse an internal edge either clockwise or counterclockwise, that is, any edge can possibly be an internal edge of at most two sequential cycles. This is because any sequential cycle is already uniquely determined only by specifying one of its internal edges and the direction in which this edge is traversed by the cycle (i.e., either clockwise or counterclockwise). In other words, two sequential cycles that share an internal edge traversed by these two cycles in the same direction must necessarily coincide since the walk around the cycle is unambiguously determined by alternating the left and right turns. Thus, starting with an arbitrary internal edge that we traverse either clockwise or counterclockwise, we go on along a corresponding tristrip by alternating the left and right turns. This tristrip may end up in a boundary edge of the surface, or it may terminate before some edge would be traversed twice by this tristrip, both clockwise and counterclockwise, which is not allowed since by definition one tristrip may encode only different triangles. The last possibility is that following this tristrip, we come back to the initial edge, which is traversed along the tristrip solely clockwise or solely counterclockwise. In this case, the tristrip is properly cycled (encoding different triangles) and represents one sequential cycle, which is included in C. Hence, C can be obtained by repeating this procedure until all internal edges are traversed both clockwise and counterclockwise (along different tristrips). Clearly, the computational time that is needed for generating C is proportional to the number of edges in T, which is linear in terms of n.

In addition, we will assign a unique representative internal edge $e_c \in I_c$ to each sequential cycle $c \in C$ in T by using the following (linear time) algorithm, in which $R \subseteq C$ denotes the set of sequential cycles to which their representative edges have already been assigned in the course of computation:

1. $R := \emptyset$
2. **while** $R \neq C$ **do**
   (a) choose any cycle $c \in C \setminus R$
   (b) choose any edge from I_c to be the representative edge e_c of c
   (c) $R := R \cup \{c\}$
   (d) **while** $(\exists\, c' \in C \setminus R)\ \ (e_c \in I_c \cap I_{c'})$ **do**
      i. choose any edge from $I_{c'} \setminus \{e_c\}$ to be the representative edge $e_{c'}$ of c'
      ii. $R := R \cup \{c'\}$
      iii. $c := c'$

This procedure guarantees that no representative edge is assigned to two cycles at the same time. Indeed, if a representative edge e_c is assigned to some sequential cycle $c \in C$ for the first time, which is done in step 2b or 2d(i), then this edge can possibly be an internal edge of at most one other sequential cycle $c' \in C$, that is, $e_c \in I_c \cap I_{c'}$. In such a case, when condition of **while** statement 2d is satisfied, a representative edge $e_{c'}$ different from e_c is assigned to c' in step 2d(i). Hence, the edge e_c can only be a representative edge of one cycle c.

3.2 The Construction of Hopfield Network $\mathcal{H}_T$. In this section, we describe the construction of a Hopfield network $\mathcal{H}_T$, which is used for generating the stripifications for a given triangulation T. The Hopfield network $\mathcal{H}_T$ is composed of two parts corresponding to a disjoint partition $N = N_1 \cup N_2$ of the set of neurons in $\mathcal{H}_T$. The first part of $\mathcal{H}_T$, which basically encodes tristrips of a stripification Σ, contains two neurons ℓ_e and r_e for each internal edge $e \in I$ in T,

$$N_1 = \{\ell_e, r_e \,|\, e \in I\}\,. \tag{3.1}$$

In particular, two triangles in T that share an internal edge e are connected in a tristrip $\sigma \in \Sigma$ if and only if a corresponding neuron either ℓ_e or r_e is active, which also indicates that the underlying tristrip σ traverses edge e either counterclockwise ($y_{\ell_e} = 1$) or clockwise ($y_{r_e} = 1$), respectively. The architecture of the first part of $\mathcal{H}_T$ (specified below) ensures that the Hopfield network $\mathcal{H}_T$ converges to the states that encode disjoint correct tristrips, which alternate left and right turns. The second part of $\mathcal{H}_T$, on the other hand, contains two neurons a_c and d_c for each sequential cycle $c \in C$ in T:

$$N_2 = \{a_c, d_c \,|\, c \in C\}\,. \tag{3.2}$$

The purpose of this part is to prevent $\mathcal{H}_T$ from converging to the states that encode cycled strips of triangles along the sequential cycles that appear in

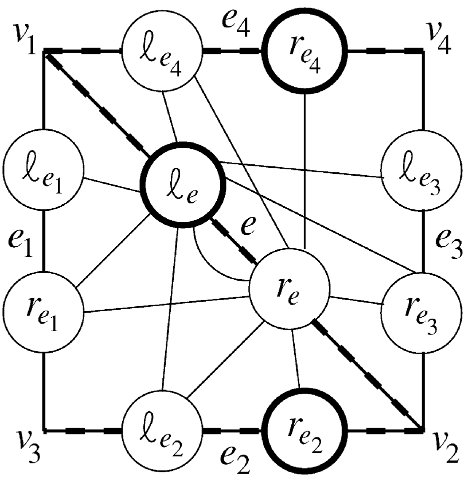

Figure 3: Construction of $\mathcal{H}_T$ related to $e \in I$.

the triangulation T (Estkowski et al., 2002). As follows from the analysis in section 4, such infeasible states must be excluded because their energy given by equation 2.2 is less than those encoding the optimal stripifications.

We now specify the architecture of the first part of $\mathcal{H}_T$ in detail. Let $e = \{v_1, v_2\} \in I$ be an internal edge in T and $L_e = \{e, e_1, e_2, e_3, e_4\}$ with $e_1 = \{v_1, v_3\}$, $e_2 = \{v_2, v_3\}$, $e_3 = \{v_2, v_4\}$, and $e_4 = \{v_1, v_4\}$ denote the set of edges of the two triangles $\{v_1, v_2, v_3\}$ and $\{v_1, v_2, v_4\}$ that share this edge e (see Figure 3). Furthermore, denote by $J_e = \{\ell_f, r_f \mid f \in L_e \cap I\}$ the set of neurons that are associated with the internal edges from L_e. In the Hopfield network $\mathcal{H}_T$, unit ℓ_e is connected by negative weights with all neurons from J_e except for units r_{e_2} (if $e_2 \in I$), ℓ_e, and r_{e_4} (if $e_4 \in I$) whose states may encode a tristrip $\sigma \in \Sigma$ that traverses edge e counterclockwise. In particular, if neuron ℓ_e is active ($y_{\ell_e} = 1$), then these negative weights ensure that the neurons in

$$J_{\ell_e} = J_e \setminus \left\{r_{e_2}, \ell_e, r_{e_4}\right\} \tag{3.3}$$

connected to ℓ_e are passive (i.e., $y_i = 0$ for $i \in J_{\ell_e}$), which locally forces the tristrip σ to alternate the left and right turns and allows σ to continue through internal edges e_2, e_4 clockwise. Such a situation (for $L_e \subseteq I$) is depicted in Figure 3, where the edges shared by consecutive triangles of σ are marked together with the associated active neurons r_{e_2}, ℓ_e, r_{e_4}. Similarly, unit r_e is connected with the neurons from

$$J_{r_e} = J_e \setminus \left\{\ell_{e_1}, r_e, \ell_{e_3}\right\}, \tag{3.4}$$

which may encode a tristrip that traverses edge e clockwise. Recall that any internal edge is shared by exactly two triangles, and hence our construction in Figure 3 covers any complex triangulation T. Thus, for each internal edge $e \in I$, define the symmetric weights of neurons from N_1 as

$$\begin{aligned} w(i, \ell_e) = w(\ell_e, i) &= -7 \quad \text{for } i \in J_{\ell_e}, \\ w(i, r_e) = w(r_e, i) &= -7 \quad \text{for } i \in J_{r_e}, \end{aligned} \tag{3.5}$$

which ensures that the Hopfield network $\mathcal{H}_T$ converges to the states that encode correct stripifications of T.

Furthermore, for each representative edge e_c corresponding to a unique sequential cycle $c \in C$, denote by j_c one of the two neurons associated with e_c, namely, $j_c = \ell_{e_c}$, if the cycled tristrip c traverses e_c counterclockwise, or $j_c = r_{e_c}$ if c traverses e_c clockwise. Let $J = \{j_c \mid c \in C\}$ be the set of all such units, whereas $J' = N_1 \setminus J$ contains the remaining neurons in the first part of $\mathcal{H}_T$. We can now define the thresholds of neurons from $N_1 = J \cup J'$ as

$$h(j) = \begin{cases} 1 + 2b_{e(j)} & \text{for } j \in J \\ -5 + 2b_{e(j)} & \text{for } j \in J' \end{cases}, \tag{3.6}$$

where $e(j) = e$ denotes an internal edge that unit $j \in \{\ell_e, r_e\}$ is associated with, and b_e $(e \in I)$ is the number of sequential cycles $c \in C$ whose boundary B_c excluding L_{e_c} contains edge e, that is, $b_e = |\{c \in C \mid e \in B'_c\}|$ where $B'_c = (B_c \cap I) \setminus L_{e_c}$ is the set of internal edges that create the boundary of sequential cycle c excluding the edges in L_{e_c}. Obviously $b_e \leq 2$ since any edge can possibly be a boundary edge of at most two sequential cycles. This is because any edge e is shared by at most two triangles, and the two other edges in each of these triangles may belong only to the internal edges of one sequential cycle that has e as its boundary edge since by traversing one of these two edges in the direction that avoids the other one, we could possibly produce a sequential cycle, which, however, has e as an internal edge.

The architecture of the second part of the Hopfield network $\mathcal{H}_T$, whose purpose is to avoid the states of $\mathcal{H}_T$ encoding the cycled tristrips, will now be defined (see Figure 4). Each neuron d_c $(c \in C)$ in N_2 computes the disjunction (OR) of Boolean outputs from all the neurons $i \in N_1$ associated with boundary edges $e(i) \in B'_c$ of sequential cycle c (except for the edges of L_{e_c}). As outlined in Figure 4, this is implemented by the following (symmetric) weights and threshold for each sequential cycle $c \in C$:

$$w(i, d_c) = w(d_c, i) = 2 \quad \text{for all } i \in N_1 \text{ such that } e(i) \in B'_c, \tag{3.7}$$

$$h(d_c) = 1. \tag{3.8}$$

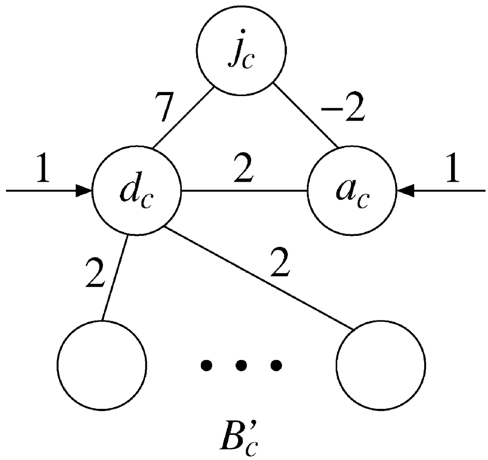

Figure 4: Construction of $\mathcal{H}_T$ related to $c \in C$.

Furthermore, only if this neuron d_c is active is the activation of unit j_c from N_1 associated with the representative edge e_c enabled by using the positive (symmetric) weight defined for each $c \in C$:

$$w(d_c, j_c) = w(j_c, d_c) = 7. \tag{3.9}$$

For the passive neuron d_c, on the other hand, unit $j_c \in J$ stays passive due to its positive threshold 3.6. Hence, any tristrip σ may then traverse edge e_c along the sequential cycle c ($y_{j_c} = 1$) only if some boundary edge $e(i) \in B'_c$ of c is traversed by another tristrip σ' ($y_i = 1$) crossing the sequential cycle c. This ensures that the tristrip σ is not cycled along c since it is cut by tristrip σ'. Thus, the states of Hopfield network $\mathcal{H}_T$ do not encode cycled tristrips. In addition, unit a_c balances the contribution of active d_c to the energy 2.2 when j_c is passive. As depicted in Figure 4, this is implemented by the following symmetric weights and threshold for each $c \in C$:

$$w(d_c, a_c) = w(a_c, d_c) = 2, \quad w(j_c, a_c) = w(a_c, j_c) = -2, \tag{3.10}$$

$$h(a_c) = 1. \tag{3.11}$$

This completes the construction of the Hopfield network $\mathcal{H}_T$.

Moreover, observe that the number of units $s = |N_1| + |N_2| = 2|I| + 2|C| = O(n)$ in $\mathcal{H}_T$ given by definitions 3.1 and 3.2 is linear in terms of triangulation size $n = |T|$ because the number of sequential cycles $|C|$ can be upper-bounded by $2|I| = O(n)$ since each internal edge can be traversed by at most two sequential cycles. Similarly, the number of connections in $\mathcal{H}_T$ can be upper-bounded by $7 \cdot 2|I| + 2 \cdot 2|I| + 3|C| = O(n)$ according to equations 3.5, 3.7, and 3.9 to 3.10, respectively, since each internal edge may appear in B_c for at most two $c \in C$. Clearly, the reduction can also be done within linear time $O(n)$ since the thresholds and symmetric weights are first computed for the neurons in N_1 by formula 3.6 and by formula 3.5 for every internal edge in I, respectively, and then for the units in N_2 by formulas 3.7 to 3.11 for every sequential cycle in C.

4 The Correctness of the Reduction

The correctness of the reduction introduced in section 3 will be verified by proving theorem 1 below. Let $\mathcal{S}_T$ be the set of optimal stripifications with the minimum number of tristrips for T. Define $\Sigma \in \mathcal{S}_T$ as equivalent to $\Sigma' \in \mathcal{S}_T$ if their corresponding tristrips encode the same sets of triangles: $\Sigma \sim \Sigma'$ iff $\{T_\sigma \mid \sigma \in \Sigma\} = \{T_{\sigma'} \mid \sigma' \in \Sigma'\}$. For example, two equivalent optimal stripifications may differ in a tristrip σ encoding the triangles of a sequential cycle $c \in C$ ($T_\sigma = T_c$), which is split at two different positions. Moreover, let $[\Sigma]_\sim = \{\Sigma' \in \mathcal{S}_T \mid \Sigma' \sim \Sigma\}$ be the class of optimal stripifications equivalent to $\Sigma \in \mathcal{S}_T$, and denote by $\mathcal{S}_T/_\sim = \{[\Sigma]_\sim \mid \Sigma \in \mathcal{S}_T\}$ the partition of $\mathcal{S}_T$ into these equivalence classes.

Theorem 1. *Let $\mathcal{H}_T$ be a Hopfield network corresponding to a triangulation T with n triangles and denote by $Y^* \subseteq \{0, 1\}^s$ the set of all stable states that can be reached during sequential computation by $\mathcal{H}_T$ starting at the zero initial state. Then each state $\boldsymbol{y} \in Y^*$ encodes a correct stripification $\Sigma_{\boldsymbol{y}}$ of T and has energy*

$$E(\boldsymbol{y}) = 5(k - n) \tag{4.1}$$

where k is the number of tristrips in $\Sigma_{\boldsymbol{y}}$. In addition, there is a one-to-one correspondence between the classes of equivalent optimal stripifications $[\Sigma]_\sim \in \mathcal{S}_T/_\sim$ having the minimum number of tristrips for T and the states in Y^* with the minimum energy $min_{\boldsymbol{y}\in Y^*} E(\boldsymbol{y})$.

Proof. Particular statements of the theorem are proven in the following three sections.

4.1 The States in Y^* Encode Correct Stripifications. The stripification $\Sigma_{\mathbf{y}}$ is decoded from $\mathbf{y} \in Y^*$ as follows. Denote by $I_0 = \{e \in I \mid y_{\ell_e} = y_{r_e} = 0\}$ the set of internal edges $e \in I$ whose associated neurons ℓ_e, r_e are both passive while its complement $I_1 = I \setminus I_0$ is composed of the internal edges with one of the two associated neurons being active (we will prove below that either $y_{\ell_e} = 1$ or $y_{r_e} = 1$). Then each ordered sequence $\sigma = (v_1, \ldots, v_m)$ of $m \geq 3$ vertices that encodes $n(\sigma) = m - 2$ different triangles $\{v_p, v_{p+1}, v_{p+2}\} \in T$ for $1 \leq p \leq m - 2$ whose edges $e_0 = \{v_1, v_3\}$, $e_m = \{v_{m-2}, v_m\}$, and $e_p = \{v_p, v_{p+1}\}$ for $1 \leq p \leq m - 1$ satisfy $e_0, e_1, e_{m-1}, e_m \in I_0 \cup B$ and $e_2, \ldots, e_{m-2} \in I_1$, is included in $\Sigma_{\mathbf{y}}$. Notice that $\sigma \in \Sigma_{\mathbf{y}}$ with

$n(\sigma) = 1$ encodes a single triangle with all its edges in $I_0 \cup B$. It will be proven that $\Sigma_{\mathbf{y}}$ corresponding to a stable state $\mathbf{y} \in Y^*$ is a correct stripification of T.

We first observe that for every active neuron $j \in N_1$ ($y_j = 1$), all the units $i \in J_j$ are passive ($y_i = 0$), where J_j is defined in equations 3.3 and 3.4. In particular, for each unit $j \in N_1 = J \cup J'$, the number of positive weights 3.7 contributing to its excitation ξ_j is at most $b_{e(j)}$, and these are subtracted within threshold $h(j)$ according to equation 3.6. Hence, if all the units $i \in J_j$ are passive, then $\xi_j \leq 5$ for $j \in J'$ due to equation 3.6, whereas $\xi_j \leq 6$ for $j \in J$ may include positive weight 3.9. Thus, any active unit $i \in J_j$ contributing to ξ_j via negative weight 3.5 makes unit j passive. By the construction of $\mathcal{H}_T$, this guarantees that sets T_σ for $\sigma \in \Sigma_{\mathbf{y}}$ are pairwise disjoint and that each $\sigma \in \Sigma_{\mathbf{y}}$ encodes different triangles whose shared edges follow alternating left and right turns.

Further, it must also be checked that the stripification $\Sigma_{\mathbf{y}}$ covers all triangles in T: $\bigcup_{\sigma \in \Sigma_{\mathbf{y}}} T_\sigma = T$. Any triangle in T either creates a trivial tristrip σ with $n(\sigma) = 1$ when all its edges are in $I_0 \cup B$, or it is connected to a tristrip (at least one of its edges is in I_1). The only problematic case that must be avoided would appear when this tristrip is cycled, which means that such a tristrip would not satisfy, for example, $e_1 \in I_0 \cup B$ in the definition of $\Sigma_{\mathbf{y}}$. Thus, according to the definition of $\Sigma_{\mathbf{y}}$, it suffices to prove that there is no sequential cycle $c = (v_1, \ldots, v_m)$ (recall $v_{m-1} = v_1$, $v_m = v_2$) such that $e_p = \{v_p, v_{p+1}\} \in I_1$ for every $p = 1, \ldots, m-2$. Suppose on the contrary that such $c \in C$ exists, which implies $B_c \cap I \subseteq I_0$. Then the unit $j_c \in J$ associated with its representative edge $e_c = e_q$ for some $1 \leq q \leq m-2$ could not be activated during sequential computation of $\mathcal{H}_T$ starting at the zero state (i.e., $y_{j_c}^{(t)} = 0$ for any $t \geq 0$) since its positive threshold $h(j_c)$ defined in equation 3.6 can be reached only by weight 3.9 from d_c. However, d_c computes the disjunction of outputs from the neurons $i \in N_1$ associated with $e(i) \in B_c' \subseteq I_0$ according to equations 3.7 and 3.8, which are passive in the course of computation. Hence, $y_{d_c}^{(t)} = 0$ for $t \geq 0$, making unit a_c also passive. Thus, $e_q \in I_0$, which is a contradiction. This completes the argument for $\Sigma_{\mathbf{y}}$ to be a correct stripification of T.

4.2 The Energy of States in Y^*. Assume that $\Sigma_{\mathbf{y}}$ contains k tristrips. From the definition of $\Sigma_{\mathbf{y}}$, each tristrip $\sigma \in \Sigma_{\mathbf{y}}$ is encoded using the active neurons associated with $n(\sigma) - 1$ edges from I_1. Hence, the number of active units in N_1 is

$$|I_1| = \sum_{\sigma \in \Sigma_{\mathbf{y}}} (n(\sigma) - 1) = n - k. \tag{4.2}$$

We will show that each active neuron $j \in N_1$ is accompanied by a contribution of -5 to the energy 2.2, which gives formula 4.1 according to equation 4.2. Assume that a neuron $j \in N_1 = J' \cup J$ is active, which implies

$y_i = 0$ for every unit $i \in J_j$. Moreover, neuron j is connected to $b_{e(j)}$ units d_c for $c \in C$, such that $e(j) \in B'_c$, which are active because the underlying disjunctions include active j. Consider first the case when the active neuron j is from J', which produces the following contribution to the energy:

$$\begin{aligned}
&-\frac{1}{2}b_{e(j)}w(d_c, j) - \frac{1}{2}b_{e(j)}w(j, d_c) + h(j) \\
&= -b_{e(j)}w(d_c, j) + h(j) \\
&= -2b_{e(j)} - 5 + 2b_{e(j)} = -5,
\end{aligned} \tag{4.3}$$

according to equations 2.2, 3.6, and 3.7. Similarly, the active neuron $j = j_{c_1}$ from J for some $c_1 \in C$ assumes active d_{c_1} and makes a_{c_1} passive due to equations 3.10 and 3.11, which contributes to the energy

$$\begin{aligned}
&-b_{e(j)}w(d_c, j) - w\left(d_{c_1}, j_{c_1}\right) + h(j) + h\left(d_{c_1}\right) \\
&= -2b_{e(j)} - 7 + 1 + 2b_{e(j)} + 1 = -5
\end{aligned} \tag{4.4}$$

according to equations 3.6 to 3.9. In addition, unit a_c for any $c \in C$ balances the contribution of active neuron d_c to the energy when j_c is passive, that is,

$$-w(a_c, d_c) + h(d_c) + h(a_c) = -2 + 1 + 1 = 0 \tag{4.5}$$

according to equations 3.8, 3.10, and 3.11.

4.3 One-to-One Correspondence. We show that for any optimal stripification $\Sigma \in \mathcal{S}_T$, there is one state $\mathbf{y} \in Y^*$ of $\mathcal{H}_T$ such that $\Sigma \in [\Sigma_{\mathbf{y}}]_\sim$. An optimal stripification Σ' equivalent to Σ is used to determine this state $\mathbf{y}$ so that $\Sigma' = \Sigma_{\mathbf{y}}$. In particular, for each tristrip $\sigma \in \Sigma$ that encodes triangles $T_\sigma = T_c$ of some sequential cycle $c \in C$, define a corresponding tristrip $\sigma' = (v_1, \ldots, v_m) \in \Sigma'$ so that $T_{\sigma'} = T_\sigma$ and σ' starts and terminates with the representative edge $e_c = \{v_1, v_2\} = \{v_{m-1}, v_m\}$ of c. Now we can define the state $\mathbf{y}$ of $\mathcal{H}_T$ as follows. For each $e \in I$, either ℓ_e or r_e is active iff there exists a tristrip $\sigma = (v_1, \ldots, v_m) \in \Sigma'$ traversing the edge $e = \{v_p, v_{p+1}\}$ for some $2 \le p \le m-2$ counterclockwise or clockwise, respectively. In addition, for each $c \in C$, unit d_c is active iff there is an active neuron $i \in N_1$ associated with $e(i) \in B'_c$, whereas unit a_c is active iff d_c is active and j_c is passive. Clearly, $\mathbf{y}$ is a stable state of $\mathcal{H}_T$. It must still be proven that $\mathbf{y}$ can be reached during sequential computation by $\mathcal{H}_T$ starting at the zero initial state: $\mathbf{y} \in Y^*$.

For this purpose, define a directed graph $G = (C, A)$ whose vertices are sequential cycles and $(c_1, c_2) \in A$ is an edge of G iff $e_{c_1} \in B'_{c_2}$. Let C' be the set of all the vertices $c \in C$ with $y_{j_c} = 1$ that create directed cycles in G. For a contradiction, suppose that all the units $i \in N_1$ associated with $e(i) \in \bigcup_{c \in C'} B'_c \setminus E_{C'}$ where $E_{C'} = \{e_c \mid c \in C'\}$ are passive. Notice that for each $c \in C'$, the units $i \in N_1$ associated with $e(i) \in B_c \cap L_{e_c}$ are also passive due to j_c being active. Hence, $y_i = 0$ for all $i \in N_1$ such that $e(i) \in \bigcup_{c \in C'} B_c \setminus E_{C'}$.

Such a stable state cannot be reached during any sequential computation by $\mathcal{H}_T$ starting at the zero initial state, which means $\mathbf{y} \notin Y^*$. This is because neuron j_{c_1} for any $c_1 \in C'$ can be activated only by the corresponding unit d_{c_1} whose activation depends solely on an active neuron j_{c_2} for another $c_2 \in C'$ within a directed cycle of G (i.e., $(c_2, c_1) \in A$), since the remaining neurons associated with the edges from $B'_{c_1} \setminus E_{C'}$, which represent the inputs for the disjunction computed by d_{c_1}, are passive. As $\Sigma_\mathbf{y}$ is optimal stripification, the underlying tristrips traverse the internal edges of sequential cycles from C' as much as possible, being interrupted only by edges from $\bigcup_{c \in C'} B_c \setminus E_{C'}$.

Observe that any tristrip $\sigma \in \Sigma_\mathbf{y}$ crossing some sequential cycle $c_1 \in C'$, that is, $\emptyset \neq T_\sigma \cap T_{c_1} \neq T_\sigma$, ends within this sequential cycle c_1 because σ enters c_1 only by traversing its boundary edge $e_{c_2} \in B'_{c_1}$ with $y_{j_{c_2}} = 1$, which is the only representative edge of a sequential cycle $c_2 \in C'$, which necessarily contains σ, that is, $T_\sigma \subseteq T_{c_2}$. In addition, we will prove that any sequential cycle $c \in C'$ contains at least two tristrips $\sigma_1, \sigma_2 \in \Sigma_\mathbf{y}$, that is, $T_{\sigma_1} \subseteq T_c$ and $T_{\sigma_2} \subseteq T_c$. Let $c_1, c_2 \in C'$ be sequential cycles such that $(c_1, c), (c, c_2) \in A$ are two consecutive edges within a directed cycle in G (possibly $c_1 = c_2$). The tristrip $\sigma \in \Sigma_\mathbf{y}$ that traverses the representative edge $e_{c_1} \in B'_c$ cuts the sequential cycle c ($\emptyset \neq T_\sigma \cap T_c \neq T_\sigma$) whose remaining triangles in $T_c \setminus T_\sigma$ could still be linked together in one tristrip $\sigma_1 \in \Sigma_\mathbf{y}$ so that $T_{\sigma_1} = T_c \setminus T_\sigma$. However, such a tristrip σ_1 enters the sequential cycle c_2 ($\emptyset \neq T_{\sigma_1} \cap T_{c_2} \neq T_{\sigma_1}$) by traversing the representative edge $e_c \in B'_{c_2}$, which implies $e_c \notin I_{c_1}$, and thus σ_1 terminates in c_2, which cuts σ_1 in two parts. Hence, there must be at least two tristrips $\sigma_1, \sigma_2 \in \Sigma_\mathbf{y}$ such that $T_{\sigma_1}, T_{\sigma_2} \subseteq T_c$.

Thus, a stripification $\Sigma'_\mathbf{y}$ with fewer tristrips can be constructed from $\Sigma_\mathbf{y}$ by introducing only one tristrip $\sigma^* \in \Sigma'_\mathbf{y}$ such that $T_{\sigma^*} = T_c$ (e.g., $y_{j_c} = 0$) instead of the two tristrips $\sigma_1, \sigma_2 \in \Sigma_\mathbf{y}$, and by shortening any tristrip $\sigma \in \Sigma_\mathbf{y}$ that crosses and thus ends within the sequential cycle c, to $\sigma' \in \Sigma'_\mathbf{y}$ so that $T_{\sigma'} \cap T_c = \emptyset$, which does not increase the number of tristrips. This contradicts the assumption that $\Sigma_\mathbf{y}$ is the optimal stripification, and hence $\mathbf{y} \in Y^*$. Obviously, the class of equivalent optimal stripifications $[\Sigma_\mathbf{y}]_\sim$ with the minimum number of tristrips corresponds uniquely to the state $\mathbf{y} \in Y^*$ having the minimum energy $\min_{\mathbf{y} \in Y^*} E(\mathbf{y})$ according to formula 4.1. This completes the proof of theorem 1.

Note that the reduction in theorem 1 together with the fact that the stripification problem is NP-complete (Estkowski et al., 2002) provides another NP-completeness proof for the minimum energy problem in Hopfield networks (cf. Barahona, 1982; Šíma & Orponen, 2003). In addition, the restriction to the zero initial network state in theorem 1 can sometimes be inconvenient, for example, in stochastic computation. Without this constraint, however, $\mathcal{H}_T$ may reach infeasible states. In particular, an initially active unit j_c can activate d_c in spite of $y_i = 0$ for all $i \in N_1$ such that $e(i) \in B'_c$, which admits a cycled tristrip along the sequential cycle c. Nevertheless, this can be secured by introducing the asymmetric weight $w(d_c, j_c) = 7$ for each $c \in C$ whereas $w(j_c, d_c) = 0$ (cf. equation 3.9). This revision, which is implemented in our program HTGEN and used for experiments in section 5, does not break the convergence of $\mathcal{H}_T$ to the states $\mathbf{y} \in Y^*$.

5 Experiments

5.1 Program HTGEN. An ANSI C program HTGEN (available online at http://www.cs.cas.cz/~sima/htgen-en.html) has been created to automate the reduction from theorem 1, including the simulation of the Hopfield network $\mathcal{H}_T$, using simulated annealing. The input for HTGEN is an object file (in the Wavefront .obj format)[1] describing triangulated surface model T by a list of geometric vertices with their coordinates, followed by a list of triangular faces, each composed of three vertex reference numbers. The program generates a corresponding $\mathcal{H}_T$, which then computes a stripification $\Sigma_{\mathbf{y}}$ of T. This is extracted from the final stable state $\mathbf{y} = \mathbf{y}^{(\tau^*)} \in Y^*$ of $\mathcal{H}_T$ at macroscopic time τ^* into an output .objf format file containing a list of tristrips together with vertex data (the .objf format is a variant of the Wavefront .obj format which includes a data type for tristrips).[2] The user may control the Boltzmann machine by specifying the initial temperature $T^{(0)}$ in equation 2.4 and the stopping criterion ε given as the maximum percentage of unstable units at the end of stochastic computation (the input values of ε are given in percentages, e.g., $\varepsilon = 0.1$ stands for 0.1%).

The experiments with HTGEN program were performed on a notebook HP Compaq n×6110 1.6 GHz with 512 MB RAM, running a Linux operating system. The running time, which is stated in seconds below, represents a real time exploited for overall computation including the system overhead but not including the time needed for constructing the Hopfield network $\mathcal{H}_T$ (which did not exceed 1 second in most cases).

5.2 Used Models. We have conducted experiments with the HTGEN program using 3D geometric models represented by polygonal meshes from several repositories, mostly from the Web page of Gooch.[3] The detailed characteristics of models (number of vertices, number of triangles, number of sequential cycles), together with those of corresponding Hopfield nets (number of neurons, number of connections) used in the experiments, are summarized in Table 1. In particular, we have used a suite of 13 data sets that represent a single asteroid, differing only in the level of detail corresponding to the size of the mesh (see Figure 5). The smallest data set of this suite

[1] See http://www.dcs.ed.ac.uk/home/mxr/gfx/3d/OBJ.spec for further information on the Wavefront .obj format.

[2] See http://www.cs.sunysb.edu/~stripe/ for further information on the .objf format.

[3] http://www.cs.northwestern.edu/~ago820/cs351/Models/OBJmodels/.

Table 1: Characteristics of Models Used in Experiments.

	Triangulated Mesh T			Hopfield Network $\mathcal{H}_T$	
Model	Number of Vertices	Number of Triangles	Number of Seq. Cycles	Number of Neurons	Number of Connections
Asteroid250	110	216	20	688	3544
Asteroid500	223	442	12	1350	5445
Asteroid1k	477	950	18	2886	11,757
Asteroid2.5k	1211	2418	30	7314	30,039
Asteroid5k	2422	4840	43	14,606	60,237
Asteroid10k	4916	9828	62	29,608	122,476
Asteroid20k	9902	19,800	89	59,578	246,971
Asteroid40k	19,814	39,624	126	119,124	494,550
Asteroid60k	29,798	59,592	155	179,086	743,981
Asteroid80k	39,782	79,560	179	239,038	993,437
Asteroid100k	49,649	99,294	200	298,282	1,239,987
Asteroid200k	99,467	198,930	284	597,358	2,484,945
Asteroid300k	149,802	299,600	349	899,498	3,742,939
Shuttle	476	616	0	1528	4490
F-16	2344	4592	9	13,794	48,643
Cessna	6763	7446	10	16,882	46,083
Lung	3121	6076	4	18,064	63,116
Triceratops	2832	5660	2	16,984	59,532
Roman	10,473	20,904	0	62,548	218,426
Bunny	34,834	69,451	1	208,132	727,951
Dragon	437,645	871,414	334	2,610,640	9,144,021

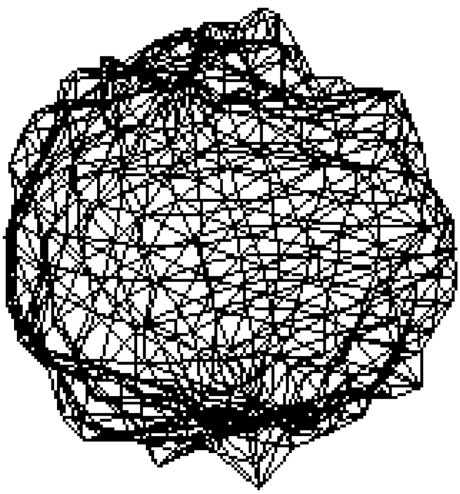

Figure 5: Asteroid1k model (950 triangles).

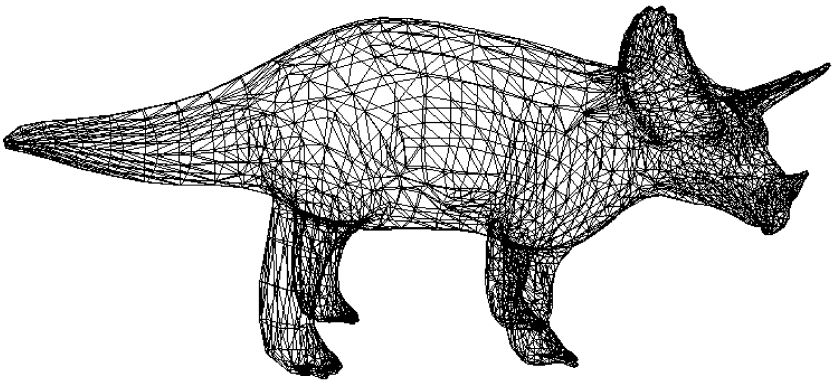

Figure 6: Triceratops model (5660 triangles).

consists of 216 triangles and the largest, 299,600 triangles. As for other models from the Web page of Gooch, we have conducted experiments with a space shuttle data set consisting of 616 triangles, two airplane data sets (F-16 and Cessna), and a lung data set; the sizes of these three models vary from 4592 to 7446 triangles. Furthermore, we have worked with the triceratops data set depicted in Figure 6 (5660 triangles), which is by Viewpoint Animation Engineering and available online from the Web page of Hu;[4] with a man figure data set, Roman (20,904 triangles) from the 3D Cafe Web Site;[5] and with a Stanford bunny data set (69,451 triangles) and a dragon data set (871,414 triangles), which are provided by Level of Detail for 3D Graphics Web Site.[6] In some cases, we had to convert a data set into the .obj format or triangulate a polygonal mesh. For the triangulation, we used part of the source code of a software package LODestar by Sainitzer and Buchegger.[7]

5.3 Number of Trials. The resulting number of tristrips obtained using HTGEN and the corresponding running times were averaged over several trials of simulated annealing. In order to justify the results of our experiments below, we first explored how the achieved stripification quality (the best number of tristrips) depends on the number of performed trials of simulated annealing. For each of three selected models, Asteroid2.5k (2418 triangles), Asteroid10k (9828 triangles), and Roman (20,904 triangles), 15 experiments have been conducted, each for a fixed number of trials; the results are summarized in Table 2. For example, during 10 trials, the best

[4] http://www.cis.uab.edu/info/grads/hux/Data/obj.html.
[5] http://www.3dcafe.com/.
[6] http://lodbook.com/models/.
[7] Available online at http://www.cg.tuwien.ac.at/research/vr/lodestar/Download/.

Table 2: Best Number of Tristrips versus Number of Trials.

	Best Number of Tristrips		
Number of Trials	Asteroid2.5k	Asteroid10k	Roman
10	244	929	2442
20	227	929	2425
30	228	897	2410
40	221	941	2405
50	228	938	2403
60	224	905	2408
70	219	908	2392
80	223	918	2412
90	220	945	2401
100	223	939	2380
200	214	935	2364
400	219	893	2395
600	208	905	2372
800	217	895	2364
1000	211	915	2380

numbers of tristrips, 244, 929, and 2442, respectively, were obtained for the underlying three models, while 223, 939, and 2380 were computed within 100 trials, and 211, 915, and 2380 were achieved after 1000 trials. It appears that after several trials, the stripification quality does not substantially increase with the increasing number of trials, and one can consider the results that are averaged over 10 to 30 trials to be reasonably reliable.

5.4 The Choice of Initial Temperature $T^{(0)}$ and Stopping Criterion ε. In the following experiment, we investigated the dependence of the resulting number of tristrips and the corresponding running time on both the initial temperature $T^{(0)}$ and the stopping criterion ε. The Asteroid40k model (39,624 triangles) is used to illustrate these dependencies, and the results are averaged over 10 trials. In particular, rows and columns in Tables 3 to 6 correspond to different values of $T^{(0)}$ and ε, respectively. Here we present only a selected window of the whole picture; many more experiments have been conducted for wider domains and more detailed scales of $T^{(0)}$ and ε (Table 6 is incomplete since the time needed for computing the underlying missing values exceeded reasonable limits). Furthermore, each cell in these tables shows the average number of tristrips over 10 trials, the minimum number of tristrips achieved in the best trial, the average real running time in seconds, and the average macroscopic time, respectively, for corresponding $T^{(0)}$ and ε. It appears that for a fixed initial temperature $T^{(0)}$ (corresponding to a row in the tables), the running time increases with decreasing ε, while the quality of resulting stripifications improves at the same time. Similarly, for a fixed ε (corresponding to a column in the tables), one can achieve better

Table 3: Dependence on the Parameters of Simulated Annealing: $\varepsilon = \mathbf{6}, \mathbf{7}, \ldots, \mathbf{17}$, $\mathbf{T^{(0)}} = \mathbf{2}, \mathbf{4}, \ldots, \mathbf{40}$, Asteroid40k (39,624 Triangles), 10 Trials.

$T^{(0)}$ \ ε	17	16	15	14	13	12	11	10	9	8	7	6	
2	11978 11869 3.2 4.0	11951 11827 3.3 4.2	11976 11914 3.2 4.2	11952 11858 3.1 4.1	11945 11854 3.0 4.2	11951 11848 3.2 4.0	11674 11611 3.9 5.0	11659 11566 3.8 5.0	11640 11567 3.8 5.0	11632 11587 3.7 5.0	11669 11605 3.7 5.0	11672 11583 3.9 5.0	
4	11030 10995 3.8 5.0	11021 10933 3.9 5.2	10995 10900 4.0 5.3	11038 10928 4.0 5.3	11057 10923 4.0 5.2	10988 10913 3.7 5.3	11032 10925 3.9 5.0	10488 10421 4.3 6.2	10487 10383 4.4 6.0	10480 10397 4.6 6.1	10455 10337 4.2 6.1	10492 10430 4.4 6.1	
6	11212 11113 3.7 5.1	11247 11108 4.1 5.5	10552 10449 4.4 6.1	10564 10460 4.6 6.2	10570 10475 4.7 6.2	10593 10528 4.5 6.1	10578 10446 4.5 6.1	**9957** **9892** **5.0** **7.0**	9984 9879 5.2 7.1	9958 9869 5.3 7.0	9485 9384 5.8 8.1	9505 9460 5.5 8.0	**10000**
8	10940 10880 4.5 6.2	10905 10752 4.9 6.4	10894 10848 4.8 6.3	10301 10235 5.2 7.1	10347 10268 5.3 7.1	10289 10166 5.1 7.2	10024 9670 5.6 7.6	9735 9682 6.0 8.1	9755 9671 5.7 8.2	9236 9171 6.4 9.1	9245 8835 6.4 9.1	8864 8767 7.1 10.1	**9000**
10	10750 10639 5.3 7.2	10742 10631 5.2 7.3	10749 10678 5.3 7.4	10209 10111 6.1 8.3	10206 10065 5.8 8.3	10005 9684 5.7 8.4	9675 9580 6.5 9.3	9420 9084 7.0 9.7	9266 9189 7.3 10.2	8874 8795 7.3 11.0	8535 8448 8.2 12.0	8169 8084 8.9 13.1	
12	10643 10535 6.1 8.2	10691 10614 6.0 8.5	10177 10088 6.4 9.3	10266 10206 6.4 9.2	9822 9711 7.1 10.1	9764 9689 7.1 10.2	9374 9309 7.8 11.2	9045 8952 8.4 12.3	8722 8527 9.3 13.1	8425 8298 9.4 14.0	8104 7913 10.6 15.1	7623 7556 11.5 17.2	**8000**
14	10677 10593 6.3 9.3	10460 10268 7.1 10.1	10341 10255 7.3 10.4	9960 9843 7.8 11.4	9606 9465 8.5 12.3	9412 9159 8.6 12.8	9121 8929 9.6 13.8	8738 8558 10.6 15.2	8438 8320 11.0 16.3	7978 7827 12.0 18.0	7569 7455 13.7 20.0	7076 6877 15.1 22.8	
16	10581 10443 7.7 10.9	10418 10342 7.8 11.3	10196 10101 8.7 12.5	9836 9761 8.9 13.1	9601 9472 9.8 14.4	9236 9095 10.5 15.6	8876 8765 11.5 17.1	8423 8319 13.1 19.2	8063 7943 13.9 21.1	7659 7581 15.5 23.3	7145 7030 17.8 26.4	6520 6413 20.9 31.0	**7000**
18	10537 10319 8.9 12.9	10232 10109 9.1 13.8	9984 9923 10.5 15.2	9676 9598 11.0 16.3	9394 9253 12.3 18.0	9043 8873 13.2 19.7	8666 8555 14.1 21.6	8233 8105 16.6 24.5	7780 7633 17.6 27.0	7243 7118 20.7 31.2	6688 6576 23.7 35.5	6093 6012 27.5 41.7	
20	10446 10373 10.6 15.5	10188 10001 11.1 16.8	9943 9821 12.6 18.4	9615 9561 13.8 20.2	9281 9141 15.1 22.5	8837 8626 17.1 25.3	8472 8358 18.3 27.8	7969 7845 20.8 31.7	7508 7425 23.7 35.8	6984 6858 26.8 41.2	6298 6125 31.9 48.3	5706 5649 37.6 57.3	**6000**
22	10440 10299 12.2 18.4	10131 9950 13.6 20.3	9855 9678 15.0 22.4	9438 9337 16.7 25.2	9106 9038 18.9 28.4	8670 8575 20.7 31.8	8242 8051 23.6 36.0	7806 7698 27.0 41.5	7248 7128 31.3 47.5	6612 6398 36.5 55.1	5977 5871 42.0 64.9	5329 5167 50.1 77.9	
24	10360 10241 15.2 22.6	10036 9934 17.0 25.1	9773 9610 18.6 28.2	9398 9276 20.3 31.4	9010 8923 23.7 35.9	8607 8538 27.1 40.6	8123 7978 30.3 47.0	7598 7504 35.3 54.0	7025 6889 40.9 62.5	6382 6220 48.3 74.2	5690 5513 56.7 87.8	4961 4811 71.2 108.3	**5000**
26	10286 10202 18.9 27.6	10050 9973 20.2 30.7	9728 9539 23.3 35.3	9328 9166 26.7 40.6	8927 8792 30.5 46.0	8527 8435 34.7 52.9	7934 7861 40.2 61.4	7434 7316 47.1 71.4	6812 6654 54.6 83.8	6186 6056 65.1 100.2	5437 5358 77.4 120.4	4675 4579 96.3 148.3	
28	10342 10238 22.2 33.8	10017 9899 26.0 38.7	9663 9526 29.6 44.5	9307 9205 33.7 51.7	8848 8803 38.7 59.3	8402 8259 45.3 69.1	7858 7718 53.2 81.3	7285 7164 61.9 95.5	6601 6506 74.1 113.2	5914 5824 87.6 134.5	5201 5080 106.1 164.2	4370 4262 134.7 205.9	
30	10262 10150 27.7 41.8	9967 9894 31.9 49.0	9651 9516 36.9 56.0	9203 9123 43.2 66.4	8803 8652 50.0 77.1	8338 8174 58.5 90.1	7758 7683 70.3 107.2	7138 6982 82.4 127.2	6489 6348 97.9 151.6	5721 5576 120.3 184.9	4985 4882 146.9 227.0	4107 4060 184.8 287.2	
32	10258 10147 34.7 52.9	9936 9868 40.5 61.7	9576 9502 47.9 72.7	9176 9097 55.6 84.3	8750 8581 65.0 99.9	8219 8157 78.8 121.3	7708 7630 93.1 143.0	7087 6922 110.6 170.8	6366 6295 134.1 206.9	5603 5521 164.3 252.5	4752 4670 202.3 311.5	3831 3705 253.5 393.6	**4000**

Table 3: (*Continued*)

$T^{(0)}$ \ ε	17	16	15	14	13	12	11	10	9	8	7	6
34	10270 10203 43.1 65.2	9922 9813 50.7 76.9	9562 9432 59.8 91.4	9172 9065 71.5 109.3	8768 8612 84.9 130.4	8219 8033 103.4 158.4	7653 7587 123.1 190.6	6966 6847 148.3 229.8	6254 6199 207.2 278.4	5404 5319 225.2 344.6	4576 4450 276.2 425.8	3629 3517 352.1 545.7
36	10240 10178 53.0 81.2	9944 9801 64.7 98.5	9533 9415 75.8 117.0	9160 9084 91.1 141.1	8731 8638 109.9 170.7	8218 8080 134.0 207.8	7589 7393 163.8 252.9	6968 6898 201.8 312.3	6191 6059 244.9 377.9	5360 5272 302.2 468.2	4412 4305 375.9 583.6	3472 3386 486.4 750.8
38	10249 10162 67.2 103.0	9923 9787 80.6 124.1	9537 9414 97.8 150.0	9156 9031 118.2 183.5	8698 8631 146.3 225.6	8176 8006 178.8 278.0	7545 7403 216.8 340.2	6876 6702 270.7 418.3	6110 6036 330.8 513.4	5242 5176 416.7 646.2	4248 4102 520.9 808.6	3303 3211 668.3 1036.7
40	10194 10064 83.3 128.5	9930 9820 101.5 156.0	9535 9443 126.0 195.6	9176 9035 154.2 238.9	8670 8581 189.6 294.4	8132 8053 236.2 366.1	7551 7420 292.5 453.5	6856 6716 366.6 566.3	6033 5893 452.2 700.7	5059 4833 564.3 874.8	4084 3913 716.1 1110.7	3161 3057 934.4 1450.5

10000 9000 8000 7000 6000 5000 4000

Note: Each cell contains the average number of tristrips, best number of tristrips, average computation time, and average macroscopic time, respectively.

stripification results by increasing $T^{(0)}$ at the cost of additional running time.

In addition, contour lines connecting the cells in the tables that represent approximately the same quality of stripification are marked in the tables. In particular, each contour line separates the cells of the table into two groups. All the cells with fewer average tristrips than associated with the contour line belong to one group; the other group consists of the cells whose average number of tristrips is greater than or equal to this number. We can observe from the shape of these contour lines that a required number of tristrips need not be achieved at all for ε greater than some upper threshold, while this number is obtained for some small $T^{(0)}$ if ε is below some lower threshold. The transition between these two extremes seems to be continuous, while smaller initial temperatures $T^{(0)}$ are sufficient for smaller ε. The shortest running time is usually achieved within this transition region closer to the lower threshold of ε, where the contour line stagnates at some level of $T^{(0)}$ (see the cells with numbers in boldface; for each contour line, only one minimum with the greatest ε is marked, although the minimum time measured with precision in seconds is actually achieved in more cases). Hence, ε can be chosen to be not much above the lower threshold where the contour line corresponding to the minimum number of tristrips saturates and the quality of stripifications scales with $T^{(0)}$ (see the column corresponding to $\varepsilon = 1$ in Table 4). Based on these observations, suitable values for ε and $T^{(0)}$ can be chosen empirically so that HTGEN achieves semioptimal stripifications within a reasonable running time.

5.5 The Average Time Complexity. We have also measured empirically how the computational time used by HTGEN depends on the model size, that is, the number of triangles. For various fixed values of

Table 4: Dependence on the Parameters of Simulated Annealing: $\varepsilon = \mathbf{1}, \mathbf{1.5}, \ldots, \mathbf{6}$, $\mathbf{T^{(0)}} = \mathbf{1.5}, \mathbf{3}, \ldots, \mathbf{30}$, Asteroid40k (39,624 Triangles), 10 Trials.

	$T^{(0)}$ \ ε	6	5.5	5	4.5	4	3.5	3	2.5	2	1.5	1	
	1.5	12076 11980 3.8 5.0	12070 12014 3.8 5.0	12095 12029 3.6 5.0	12110 12033 3.7 5.0	12126 12077 3.4 5.0	12082 12011 3.8 5.0	12108 11991 3.9 5.0	12094 11988 3.8 5.0	12058 11958 4.4 5.9	12055 11933 4.5 6.0	12033 11955 4.4 6.0	
10000	3	10774 10610 4.4 6.0	10780 10674 4.6 6.0	10809 10691 4.3 6.0	10789 10674 4.5 6.0	10750 10590 4.7 6.2	10740 10480 5.0 6.2	10518 10399 5.3 7.0	10519 10406 5.0 7.0	10534 10422 5.1 7.0	10330 10190 5.7 8.0	10254 10185 6.2 9.0	**10000**
	4.5	9964 9849 5.0 7.0	9991 9925 5.3 7.1	9972 9895 5.0 7.0	9981 9924 5.2 7.0	9639 9591 5.5 8.0	9635 9584 5.9 8.2	9390 9289 6.6 9.0	9377 9230 6.5 9.2	9154 9058 7.3 10.0	8997 8941 7.7 11.1	8598 8513 9.4 13.9	**9000**
	6	9483 9396 5.5 8.0	9515 9388 5.9 8.1	9117 9042 6.4 9.0	9126 9063 6.7 9.0	8944 8722 6.8 9.5	8831 8760 6.8 10.0	8556 8454 7.8 11.0	8328 8171 8.3 12.0	8161 8045 8.9 13.1	7814 7703 10.4 15.3	7404 7313 13.2 19.8	**8000**
9000	7.5	8833 8761 7.0 10.1	**8824** **8693** **6.8** **10.1**	8682 8413 7.0 10.5	8517 8398 8.0 11.1	8231 8170 8.1 12.0	8006 7922 9.0 13.0	7786 7694 9.7 14.0	7605 7381 10.3 15.0	7274 7221 11.5 17.1	6855 6812 14.2 20.9	6428 6278 18.4 27.1	**7000**
	9	8373 8251 8.4 11.9	8332 8178 8.5 12.0	8060 7990 8.8 13.0	**7874** **7721** **9.6** **13.9**	7682 7547 9.9 14.8	7440 7276 10.8 16.0	7173 7072 11.6 17.5	**6893** **6826** **13.0** **19.4**	6510 6412 15.0 22.7	6096 5996 18.6 27.9	5593 5510 25.0 38.0	**6000**
	10.5	8041 7931 9.3 14.0	7772 7627 10.4 15.2	7546 7409 10.8 16.1	7364 7310 11.7 17.0	7124 7035 12.1 18.4	6867 6758 13.8 19.8	6592 6523 15.0 22.1	6229 6111 16.5 25.2	5838 5712 19.4 30.0	5377 5308 24.9 38.0	4849 4788 35.0 53.4	**5000**
8000	12	7631 7513 11.4 17.1	7408 7290 12.3 18.3	7084 6892 13.2 19.9	6859 6698 14.7 21.3	6582 6433 15.5 23.1	6272 6202 17.9 26.1	**5932** **5822** **19.1** **29.1**	5605 5512 22.4 33.6	5236 5098 26.3 40.3	4784 4657 33.8 51.3	4255 4171 48.2 74.7	
	13.5	7240 7170 14.3 21.0	6939 6766 15.3 22.9	6694 6585 16.0 24.6	6372 6274 17.9 26.7	6102 6004 19.7 29.8	5794 5679 21.6 32.7	5399 5314 24.8 37.9	5030 4917 29.1 44.6	4678 4561 35.1 53.8	4234 4176 46.0 71.0	3726 3647 69.5 106.5	**4000**
7000	15	6806 6571 17.9 26.6	6551 6387 18.7 28.5	6228 6125 21.0 31.5	5954 5856 22.9 34.2	5616 5464 24.7 38.0	5247 5164 28.8 42.9	**4934** **4813** **33.0** **49.9**	4551 4494 39.3 58.9	4144 4064 48.4 74.1	3714 3605 64.8 100.1	3179 3093 99.5 155.1	
	16.5	6435 6288 22.1 33.4	6134 5987 24.5 36.1	5822 5697 25.9 39.9	5517 5452 28.5 43.5	5166 5049 32.2 49.3	4801 4599 36.8 56.8	4424 4376 42.6 65.5	4084 4007 51.2 79.3	3652 3514 65.5 100.6	3226 3105 91.8 141.2	2778 2690 142.9 222.3	**3000**
	18	6096 6011 27.8 41.7	5815 5723 30.1 45.6	5455 5403 33.0 50.4	5123 5000 36.8 56.5	4803 4715 41.8 63.7	4426 4337 48.4 73.3	4029 3925 56.6 86.8	3658 3549 68.5 106.2	3274 3215 89.5 136.7	2854 2774 124.7 192.6	2363 2281 206.3 320.6	
6000	19.5	5754 5656 35.0 53.3	5404 5328 38.1 58.6	5084 4958 42.5 64.9	4775 4684 47.8 73.6	4365 4255 53.9 82.9	4028 3921 62.4 95.6	3637 3518 75.0 115.3	3268 3195 91.7 141.5	**2835** **2759** **123.2** **188.6**	2449 2364 177.8 275.3	2050 1956 301.1 467.9	
	21	5477 5267 43.7 66.9	5095 4985 48.0 74.3	4786 4692 54.6 83.0	4431 4331 61.5 93.6	4008 3813 70.5 108.2	3642 3483 82.4 127.0	3279 3236 100.6 154.7	2893 2796 125.2 193.7	2530 2480 167.6 259.4	2129 2072 251.5 387.8	1790 1753 442.2 686.0	**2000**
	22.5	5194 5018 55.4 84.5	4846 4728 62.9 95.9	4483 4355 67.9 105.6	4085 3932 78.8 121.8	3697 3596 91.2 140.2	3329 3178 109.0 167.2	2951 2888 132.0 204.5	2616 2512 170.4 263.2	2215 2163 232.8 359.6	1875 1772 354.9 549.7	1502 1404 657.5 1018.5	

Table 4: (*Continued*)

	$T^{(0)}$ \ ε	6	5.5	5	4.5	4	3.5	3	2.5	2	1.5	1	
	24	5008 4920 70.0 108.0	4565 4492 79.2 121.8	4201 4111 88.0 136.5	3781 3596 100.4 155.6	3382 3295 117.8 183.5	3049 2951 140.9 219.4	2687 2627 175.3 272.0	2308 2223 229.9 355.7	**1965** **1882** **319.7** **497.2**	1668 1609 506.7 783.4	1304 1237 963.1 1495.9	
5000	25.5	4699 4526 89.9 137.8	4270 4193 99.4 153.2	3962 3904 112.8 175.4	3533 3484 130.7 202.0	3119 3022 153.4 236.6	2758 2681 184.4 286.1	2419 2359 233.0 362.9	2078 1990 313.4 484.2	1752 1682 442.0 686.6	1427 1340 710.1 1102.3	1112 1073 1397.4 2175.0	
	27	4480 4382 113.1 175.1	4087 4020 129.3 198.9	3695 3538 147.0 227.3	3321 3118 170.0 262.8	2914 2845 199.2 308.1	2477 2392 247.1 382.4	2138 2049 313.0 485.8	1854 1729 428.0 663.9	1560 1425 621.8 963.5	1248 1210 1017.7 1580.4	**978** **931** **2086.0** **3243.8**	**1000**
	28.5	4252 4071 145.5 224.4	3853 3738 163.9 252.5	3462 3345 186.8 288.3	3084 3035 218.8 341.3	2658 2523 265.3 410.8	2297 2207 323.5 502.2	1994 1882 414.0 645.9	1634 1545 574.6 893.8	1376 1296 859.8 1337.5	1083 976 1465.3 2273.7	807 710 3120.6 4825.9	
	30	4118 3986 183.0 282.9	3676 3555 209.0 323.2	3272 3144 241.5 372.1	2835 2683 287.0 444.0	2488 2375 343.4 535.1	2099 1971 429.1 666.4	1756 1657 564.4 876.2	1478 1376 784.9 1219.6	1227 1112 1212.6 1882.5	966 893 2108.2 3264.3	702 590 4593.4 7143.1	
		4000		**3000**			**2000**			**1000**			

Note: Each cell contains the average number of tristrips, best number of tristrips, average computation time, and average macroscopic time, respectively.

initial temperature $T^{(0)}$ and stopping criterion ε, the Boltzmann machine converged within almost a constant number of macroscopic time steps for the asteroid model meshes whose sizes were scaled from 216 up to 198,930 triangles (except for some minor fluctuations for small meshes). This is illustrated in Tables 7, 8, and 9, where the results are presented for $T^{(0)} = 5$, $\varepsilon = 0.1$, $T^{(0)} = 9$, $\varepsilon = 0.3$, and $T^{(0)} = 13$, $\varepsilon = 0.5$, respectively. These experiments provide evidence for the average linear time complexity of HTGEN since by construction, the execution of one macroscopic step depends linearly on the number of triangles in the model (see the end of section 3 for the proof).[8] When this empirical time complexity is

[8] In contrast to this mathematically proved fact, the actual average computational time in seconds presented in the next-to-the-last column of Tables 7, 8, and 9 does not create a clear straight line on the whole domain of mesh size, and the linear dependency can be observed only for the mesh size between 19,800 triangles (Asteroid20k) and 99,294 triangles (Asteroid100k). The reason for this discrepancy seems to be caused by the fact that the practical implementation running on the computer is influenced by the cache memory overhead, which drastically slows the computation for huge models. This effect can be partially weakened by using a higher-performance computer (e.g., with a larger RAM capacity), as it is also illustrated in these tables where the average computational time in seconds achieved alternatively with 2.2 GHz processor having 2 GB RAM is presented in parentheses, improving the empirical linear time dependency also for a larger mesh size of the Asteroid200k model. In addition, the actual number of sequential cycles may not increase exactly linearly with the mesh size (see Table 1) since we know only that it is bounded by a linear function. Nevertheless, our statement concerning the empirical linear time complexity relies on the measurements of average macroscopic time, which does not depend on the implementation or a particular number of sequential cycles.

Table 5: Dependence on the Parameters of Simulated Annealing: $\varepsilon = \mathbf{0.2}, \mathbf{0.3}, \ldots, \mathbf{1}$, $\mathbf{T^{(0)}} = \mathbf{1}, \mathbf{2}, \ldots, \mathbf{20}$, Asteroid40k (39,624 Triangles), 10 Trials.

	$T^{(0)}$ \ ε	1	0.9	0.8	0.7	0.6	0.5	0.4	0.3	0.2	
	1	12568 12476 4.0 4.9	12550 12486 3.9 5.0	12567 12477 3.9 5.0	12578 12496 4.0 5.0	12571 12486 3.7 4.9	12566 12439 4.2 5.6	12527 12381 4.0 5.2	12561 12458 3.9 5.5	12529 12476 4.1 5.3	
	2	11460 11396 5.0 7.0	11436 11354 4.8 7.0	11463 11356 4.7 7.0	11439 11333 5.1 7.0	11450 11400 4.9 7.0	11424 11354 5.8 8.0	11398 11273 5.7 8.0	11354 11243 6.1 8.6	11366 11197 6.8 9.3	
	3	10232 10168 6.4 9.0	10249 10175 6.3 9.1	10161 10033 6.7 9.9	10179 10103 6.9 10.0	10132 10031 7.5 10.8	10090 9996 7.9 11.3	9984 9924 8.4 12.3	9886 9766 9.5 14.2	9852 9733 11.2 16.6	**10000**
10000	4	9101 9023 8.5 12.0	9095 9014 8.7 12.7	8975 8869 9.2 13.6	8947 8810 9.8 14.3	8860 8814 10.3 15.2	8752 8630 11.4 16.8	8644 8578 13.0 19.2	8562 8449 14.7 22.0	8435 8361 17.8 27.5	**9000**
9000	5	8157 8018 10.4 15.7	8111 8016 11.4 16.7	8005 7933 12.0 17.7	7907 7862 13.0 19.0	7780 7659 13.7 21.0	7678 7543 15.2 23.2	7525 7433 17.8 27.0	7328 7248 21.3 32.8	7166 7014 27.6 42.6	**8000**
8000	6	7392 7285 13.0 19.6	7239 7142 14.9 21.6	7127 7014 15.1 22.9	7070 7018 16.5 24.6	6912 6834 18.8 28.1	6774 6668 19.9 30.7	6654 6570 24.3 37.4	6427 6373 30.1 46.1	6132 6029 41.5 63.6	**7000**
7000	7	6720 6583 16.3 24.5	6598 6507 17.7 26.6	6489 6391 19.8 29.1	6288 6144 21.2 32.3	6230 6158 23.6 35.5	6056 5904 26.7 41.0	5847 5760 32.7 49.9	5639 5584 41.1 62.9	5373 5304 58.1 89.5	**6000**
	8	6088 5992 20.6 31.0	6026 5905 21.7 33.4	5872 5822 24.3 36.2	5759 5687 25.8 40.0	5583 5515 30.2 45.6	5426 5322 35.5 54.0	5236 5110 42.0 64.9	4997 4891 55.1 85.1	4696 4563 82.3 127.8	**5000**
6000	9	5594 5521 25.8 38.2	5511 5448 26.7 41.1	5385 5317 29.8 45.6	5230 5172 33.5 50.9	5039 4968 38.2 58.9	4870 4810 46.4 71.2	4691 4567 55.5 85.7	4435 4373 73.9 114.8	4158 4071 107.9 167.5	
	10	5122 5083 31.4 47.5	4976 4888 33.1 51.1	4856 4720 38.1 57.6	4724 4619 42.6 65.8	4553 4436 50.0 76.7	4383 4276 57.0 88.6	4185 4117 73.6 114.2	3972 3890 96.8 150.7	3661 3564 149.5 234.1	**4000**
5000	11	4661 4580 38.4 59.1	4572 4497 41.9 64.8	4431 4382 47.8 74.1	4269 4203 53.4 82.3	4118 4046 63.6 98.7	3942 3856 76.4 117.5	3787 3683 95.4 147.8	3514 3423 131.1 204.2	3225 3161 203.9 320.7	
	12	4253 4151 48.1 74.4	4113 4021 54.7 84.6	4023 3915 59.5 92.7	3897 3821 69.2 106.8	3720 3662 81.5 125.3	3548 3410 95.3 148.8	3356 3270 124.9 194.4	3131 3029 172.4 269.4	2809 2749 278.6 434.8	**3000**
4000	13	**3859** **3737** **62.2** **95.9**	3758 3641 66.7 104.0	3608 3464 77.2 119.7	3480 3373 90.1 139.1	3361 3281 105.4 164.0	3191 3116 125.6 195.7	2993 2895 165.3 256.4	2772 2647 231.9 361.1	2523 2442 379.0 594.4	
	14	3529 3470 77.4 120.3	3414 3289 85.4 132.9	3289 3228 99.5 153.8	3161 3040 116.5 179.5	3010 2906 136.2 210.6	2856 2778 167.2 259.7	2659 2577 219.7 340.1	2465 2346 308.7 480.3	2211 2119 496.6 777.3	
3000	15	3175 3099 100.4 155.2	3104 3055 111.9 172.9	2965 2916 126.3 196.6	2842 2759 147.3 229.3	2717 2636 178.2 277.1	2562 2482 222.4 345.8	2403 2343 290.6 452.0	2213 2102 407.7 635.2	1967 1890 681.7 1066.1	**2000**

Table 5: (*Continued*)

	$T^{(0)}$ \ ε	1	0.9	0.8	0.7	0.6	0.5	0.4	0.3	0.2	
	16	2884 2806 126.5 196.4	2822 2769 142.3 222.3	2650 2554 164.4 254.4	2537 2496 191.3 296.9	2402 2340 231.1 361.2	2287 2182 291.8 453.8	2119 2032 375.0 585.8	1954 1837 558.0 867.1	1732 1651 938.0 1465.0	
	17	2631 2530 161.8 252.1	2549 2435 183.4 283.5	2412 2365 213.5 331.3	2298 2184 254.8 397.2	2153 2085 301.5 469.8	2036 1932 382.4 595.4	1912 1837 523.3 812.9	1736 1666 761.2 1182.9	1524 1473 1284.8 1996.9	
	18	2404 2336 210.6 326.6	2277 2202 239.8 370.8	2186 2051 274.8 427.8	2070 2002 326.9 508.8	1940 1841 401.3 627.2	1832 1696 510.7 793.4	1698 1619 704.3 1100.6	1494 1396 1013.8 1582.7	1318 1205 1737.6 2719.1	
	19	2140 2050 262.5 408.3	2061 1974 309.2 480.8	1949 1872 362.3 561.5	1866 1770 427.1 664.0	1786 1716 537.3 834.5	1662 1574 689.8 1074.7	1484 1418 944.3 1470.0	1323 1227 1402.6 2189.2	1166 1023 2485.5 3888.9	
2000	20	1938 1845 343.7 533.5	1846 1795 394.4 614.9	1764 1655 470.4 731.5	1648 1569 575.2 890.9	1565 1460 694.5 1083.3	1448 1358 918.5 1434.3	1337 1278 1235.9 1932.5	1197 1115 1930.7 2997.4	999 929 3565.4 5563.1	**1000**

1000

Note: Each cell contains the average number of tristrips, best number of tristrips, average computation time, and average macroscopic time, respectively.

confronted with the fact that the stripification problem is NP-complete in general (Estkowski et al., 2002), this suggests that there must be a rigorous, efficient approximation algorithm for this problem.

5.6 Comparing with FTSG. Program HTGEN has been compared against a leading practical system FTSG version 1.31 (Estkowski et al., 2002; Xiang et al., 1999) that computes online stripifications. Program FTSG is considered to be a reference stripification method not based on neural nets that is widely used in comparisons for evaluating newly proposed stripification algorithms (Vaněček & Kolingerová, 2007). Experiments have been conducted using six models (Shuttle, F-16, Triceratops, Lung, Cessna, Bunny) whose sizes vary from 616 to 69,451 triangles. In each experiment, program HTGEN performed 30 trials, sufficient to obtain reasonable results (see section 5.3), and the best solution has been chosen (in any case the best and average results, e.g., in Tables 3 to 9, do not differ drastically). Suitable parameters ε and $T^{(0)}$ of HTGEN were chosen for each model separately using the heuristics proposed in section 5.4 so that the resulting stripifications consist of as few tristrips as possible at the cost of a reasonable amount of time. Also, FTSG was run with its best options (the best combination of four relevant options, -bfs, -dfs, -alt, and -sgi, in addition to two implicitly used options, -opt and -sync; see Xiang et al., 1999, for a description of these options), which led to the least number of tristrips in the resulting stripification. The results of these experiments are summarized in Table 10, which shows that

Table 6: Dependence on the Parameters of Simulated Annealing: $\varepsilon = \mathbf{0.02}, \mathbf{0.04}, \ldots, \mathbf{0.2}$, $\mathbf{T^{(0)}} = \mathbf{1}, \mathbf{2}, \ldots, \mathbf{20}$, Asteroid40k (39,624 Triangles), 10 Trials.

	$T^{(0)}$ \ ε	0.2	0.18	0.16	0.14	0.12	0.1	0.08	0.06	0.04	0.02	
	1	12558 12487 3.6 5.2	12582 12531 4.1 5.4	12501 12434 3.8 5.1	12549 12486 4.0 5.2	12555 12506 3.9 5.2	12544 12475 3.7 5.2	12559 12517 4.2 5.8	12555 12386 4.5 6.0	12547 12419 4.2 6.2	12569 12497 4.4 5.9	
	2	11337 11279 6.6 9.3	11329 11265 6.7 9.4	11278 11197 6.9 9.9	11358 11264 6.9 9.9	11312 11167 7.3 10.9	11328 11223 7.4 11.1	11312 11206 8.2 11.7	11305 11234 8.6 12.8	11305 11196 9.5 14.0	11267 11186 11.1 16.5	
10000	3	9842 9736 11.2 16.7	9824 9732 12.0 17.5	9809 9749 12.2 18.0	9839 9684 12.9 19.3	9770 9713 13.6 20.4	9747 9614 15.0 22.2	9721 9633 15.8 23.6	9681 9605 18.1 27.1	9685 9601 22.5 34.0	9631 9528 29.1 44.4	**10000** **9000**
9000	4	8369 8255 18.4 27.9	8372 8256 19.1 29.1	8334 8245 20.8 31.7	8308 8211 21.9 33.3	8263 8183 24.4 36.6	8247 8172 26.3 40.7	8155 8079 30.4 47.1	8097 7982 36.1 56.3	8003 7869 45.0 70.4	7920 7805 70.1 108.8	**8000**
8000	5	7146 7052 27.9 42.9	7128 7048 29.5 45.7	7029 6951 33.1 51.2	7006 6945 35.3 54.2	6914 6826 40.3 62.4	6879 6804 45.5 70.0	6804 6686 53.1 82.4	6678 6608 66.3 102.5	6561 6466 88.3 136.4	6402 6299 146.0 230.1	**7000**
7000	6	6191 6104 40.3 61.7	6110 6021 44.2 69.1	6033 5960 50.4 77.2	5971 5908 54.1 83.2	5903 5853 60.5 94.2	5772 5662 72.8 113.3	5718 5632 86.6 135.5	5590 5526 111.9 175.5	5430 5260 157.0 243.8	5243 5126 277.2 434.3	**6000**
6000	7	5351 5267 58.5 90.6	5275 5227 62.4 97.4	5226 5191 71.4 111.4	5150 5074 80.7 123.5	5068 4999 92.4 143.3	4968 4860 109.7 170.2	4824 4758 135.5 210.2	4738 4667 178.4 279.3	4527 4468 259.5 406.6	4279 4189 479.3 752.6	**5000**
5000	8	4693 4575 81.3 127.6	4623 4518 88.3 137.4	4525 4456 103.5 159.6	4445 4365 119.3 184.6	4388 4300 137.1 214.6	4258 4224 165.0 258.7	4137 4059 210.5 328.0	3987 3922 275.9 432.0	3758 3641 427.3 674.8	3496 3428 878.1 1384.1	**4000**
	9	4160 4060 109.7 171.4	4046 3995 123.1 193.0	3964 3905 138.5 216.6	3906 3827 158.8 251.1	3804 3724 192.6 300.5	3675 3616 230.6 362.2	3553 3447 297.1 467.7	3391 3316 431.9 679.7	3192 3088 672.0 1056.3	2859 2745 1550.0 2436.4	**3000**
4000	10	3652 3598 150.0 233.5	3563 3370 169.8 266.4	3520 3436 192.4 300.0	3413 3333 222.2 347.0	3295 3241 273.3 428.1	3138 3018 326.1 509.5	3022 2909 440.6 692.7	2878 2831 619.6 972.8	2644 2595 1008.5 1586.7	2346 2238 2232.6 3497.2	
	11	3196 3054 203.2 319.3	3154 3063 229.5 359.3	3042 2965 272.2 425.5	2986 2909 315.3 495.9	2920 2839 373.5 583.9	2753 2695 471.8 740.8	2648 2576 598.6 939.7	2463 2368 875.9 1377.5	2242 2126 1614.2 2531.2	1920 1811 3909.0 6146.2	**2000**
3000	12	2848 2768 284.9 446.5	2797 2714 316.3 494.6	2711 2628 356.0 558.6	2630 2546 426.3 669.2	2511 2444 502.7 793.4	2392 2320 633.7 997.4	2270 2189 875.1 1375.2	2133 2053 1206.2 1892.2	1906 1817 2233.5 3513.7	1627 1490 5894.7 9280.3	
	13	2508 2458 363.1 568.6	2476 2318 428.4 670.6	2377 2305 475.0 746.0	2306 2216 574.3 900.5	2204 2111 701.5 1100.2	2095 1978 900.2 1414.0	2005 1884 1181.7 1858.5	1818 1746 1785.3 2808.2	1653 1533 3143.7 4951.9		
	14	2224 2125 508.9 796.3	2129 2057 568.7 892.5	2052 1959 658.7 1031.5	2014 1900 770.5 1208.5	1903 1812 992.0 1560.0	1813 1760 1246.7 1955.9	1698 1559 1654.5 2599.5	1571 1407 2560.0 4018.8			
2000	15	1942 1842 678.6 1063.1	1880 1821 779.0 1220.9	1795 1740 930.0 1458.9	1759 1684 1085.9 1703.3	1701 1633 1329.6 2085.0	1610 1513 1679.7 2642.2	1492 1397 2480.6 3898.3				

Table 6: (*Continued*)

$T^{(0)}$ \ ε	0.2	0.18	0.16	0.14	0.12	0.1	0.08	0.06	0.04	0.02
16	1701 1659 930.2 1451.0	1708 1656 1045.6 1635.2	1594 1552 1287.1 2018.8	1563 1458 1542.6 2415.6	1460 1361 1887.2 2956.0	1420 1368 2432.7 3816.0				
17	1515 1445 1279.2 2003.5	1469 1334 1467.9 2297.9	1400 1321 1769.2 2780.7	1347 1279 2174.9 3406.4	1291 1231 2722.9 4272.5					
18	1334 1257 1706.1 2660.1	1270 1165 2025.1 3169.4	1241 1170 2454.7 3846.4	1162 1026 2892.3 4542.7						
19	1167 1115 2435.7 3809.2	1130 1090 2865.3 4479.7	1070 898 3481.5 5451.9							
20	1006 901 3424.2 5339.0	971 919 3944.2 6172.4	**1000**							

1000

Note: Each cell contains the average number of tristrips, best number of tristrips, average computation time, and average macroscopic time, respectively.

one can achieve much better results by HTGEN than by using FTSG with its most successful options (typically -dfs, -alt; Xiang et al., 1999), although the running time of HTGEN (averaged over the 30 trials to keep this table consistent with the previous ones) grows rapidly when the global optimum is being approached. Moreover, for the F-16 and Triceratops models, the stripification results obtained by HTGEN and FTSG are graphically depicted in Figures 7, 8, and 9, 10, respectively, where the superiority of HTGEN over FTSG in the average length of tristrips is clearly visible. As concerns the time complexity, system HTGEN cannot compete with real-time program FTSG providing the stripifications within a few tens of milliseconds. Nevertheless, HTGEN can be useful if one is interested in the stripification with a small number of tristrips that may be computed at the preprocessing stage.

5.7 Huge Models. In the last experiment whose results are presented in Table 11, program HTGEN has been tested on huge models (Asteroid300k, Dragon) with hundreds of thousands of triangles, for which only three trials were performed for $\varepsilon = 0.3$ and $T^{(0)} = 10$. It appears that the stripifications better than those obtained using FTSG with its optimal options (e.g. 133,072 tristrips within 7 seconds for the Dragon model) were still achieved in a doable time frame.

Table 7: Empirical Average Time Complexity: 100 Trials, $\varepsilon = 0.1$, $T^{(0)} = 5$.

Model	Number of Triangles	Best Number of Tristrips	Average Number of Tristrips	Average Tristrip Length	Average Computational Time in Seconds (on Higher-Performance Computer)[a]		Average Macroscopic Time
Asteroid250	216	31	39	6.97	0.06	(0.04)	79.98
Asteroid500	442	67	82	6.60	0.06	(0.06)	45.14
Asteroid1k	950	151	171	6.29	0.22	(0.15)	59.69
Asteroid2.5k	2418	397	429	6.09	0.76	(0.52)	62.67
Asteroid5k	4840	808	853	5.99	2.03	(1.47)	67.43
Asteroid10k	9828	1633	1711	6.02	5.45	(3.89)	68.17
Asteroid20k	19,800	3342	3435	5.92	15.32	(10.69)	70.26
Asteroid40k	39,624	6720	6868	5.90	45.51	(25.81)	70.41
Asteroid60k	59,592	10,090	10,327	5.91	84.39	(47.61)	69.51
Asteroid80k	79,560	13,525	13,757	5.88	132.88	(74.34)	70.35
Asteroid100k	99,294	16,995	17,176	5.84	184.62	(104.49)	70.07
Asteroid200k	198,930	34,109	34,400	5.83	520.39	(293.51)	70.25

[a]See note 8.

Table 8: Empirical Average Time Complexity: 80 Trials, $\varepsilon = 0.3$, $T^{(0)} = 9$.

Model	Number of Triangles	Best Number of Tristrips	Average Number of Tristrips	Average Tristrip Length	Average Computational Time in Seconds (on Higher-Performance Computer)[a]		Average Macroscopic Time
Asteroid250	216	18	27	12.00	0.11	(0.08)	159.35
Asteroid500	442	43	58	10.28	0.14	(0.09)	88.54
Asteroid1k	950	86	114	11.05	0.40	(0.26)	106.62
Asteroid2.5k	2418	255	280	9.48	1.38	(0.98)	113.84
Asteroid5k	4840	518	556	9.34	3.51	(2.39)	116.59
Asteroid10k	9828	1052	1114	9.34	9.20	(6.26)	114.76
Asteroid20k	19,800	2148	2237	9.22	24.82	(17.29)	114.45
Asteroid40k	39,624	4347	4451	9.12	73.09	(40.46)	113.53
Asteroid60k	59,592	6550	6690	9.10	136.74	(75.91)	112.86
Asteroid80k	79,560	8650	8898	9.20	212.34	(118.80)	113.06
Asteroid100k	99,294	10,884	11,110	9.12	296.31	(167.10)	112.94
Asteroid200k	198,930	21,994	22,257	9.04	818.58	(465.71)	111.65

[a]See note 8.

Table 9: Empirical Average Time Complexity: 50 Trials, $\varepsilon = 0.5$, $T^{(0)} = 13$.

Model	Number of Triangles	Best Number of Tristrips	Average Number of Tristrips	Average Tristrip Length	Average Computational Time in Seconds (on Higher-Performance Computer)[a]		Average Macroscopic Time
Asteroid250	216	12	21	18.00	0.28	(0.20)	392.76
Asteroid500	442	26	43	17.00	0.28	(0.18)	180.60
Asteroid1k	950	72	88	13.19	0.72	(0.48)	191.00
Asteroid2.5k	2418	188	208	12.86	2.38	(1.66)	199.72
Asteroid5k	4840	355	405	13.63	6.04	(4.36)	199.76
Asteroid10k	9828	762	808	12.90	16.18	(11.16)	200.94
Asteroid20k	19,800	1535	1605	12.90	44.86	(30.24)	204.48
Asteroid40k	39,624	3047	3204	13.00	127.64	(72.44)	197.92
Asteroid60k	59,592	4653	4784	12.81	239.30	(132.98)	198.16
Asteroid80k	79,560	6217	6365	12.80	370.70	(206.38)	197.16
Asteroid100k	99,294	7802	7965	12.73	517.62	(286.70)	197.08
Asteroid200k	198,930	15,595	15,923	12.76	1424.80	(816.38)	194.98

[a]See note 8.

Table 10: Comparing HTGEN Against FTSG.

		HTGEN (30 Trials)					FTSG	
Model	Number of Triangles	ε	$T^{(0)}$	Best Number of Tristrips	Average Computational Time (s)	Average Macroscopic Time	Options	Number of Tristrips
Shuttle	616	0.12	17	95	2.70	1588.67	-dfs -alt	145
F-16	4592	0.6	26	312	197.57	7192.13	-dfs -alt	478
Triceratops	5660	0.2	20	557	286.33	7915.13	-bfs	960
Lung	6076	0.14	19	613	428.03	10,940.00		857
Cessna	7446	0.5	19	1249	241.17	6712.93	-dfs -alt	1459
Bunny	69,451	0.7	23	4404	4129.93	2748.20	-dfs -alt	6191

Figure 7: Program: HTGEN, model: F-16, number of tristrips: 312.

Figure 8: Program: FTSG, model: F-16, number of tristrips: 478.

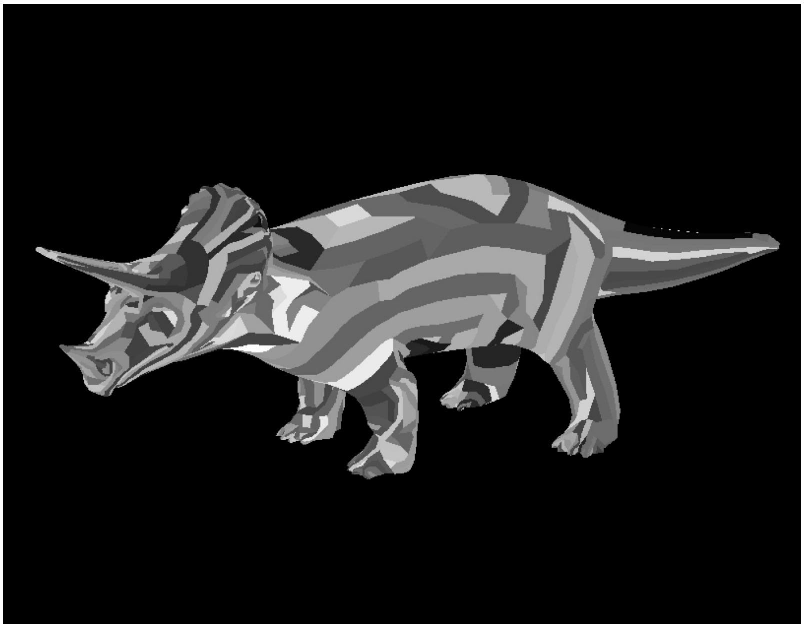

Figure 9: Program: HTGEN, model: Triceratops, number of tristrips: 557.

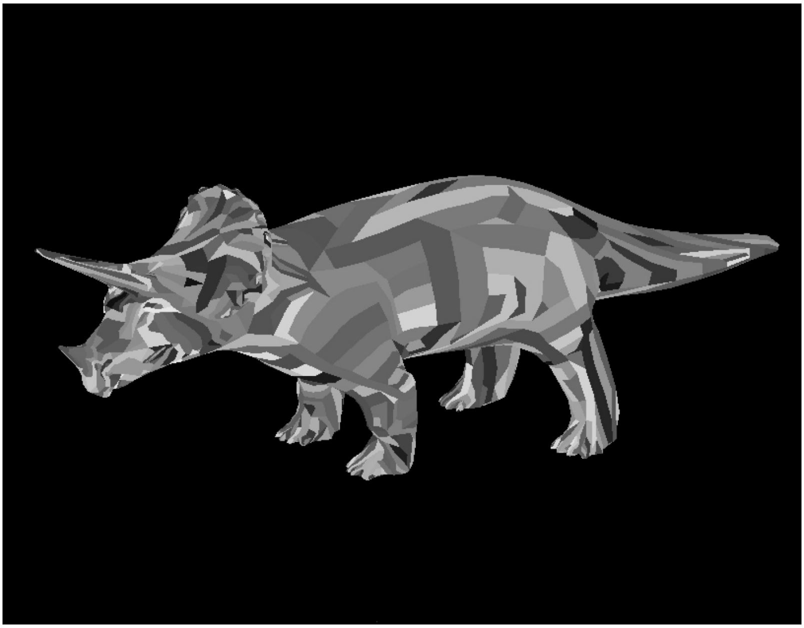

Figure 10: Program: FTSG, model: Triceratops, number of tristrips: 960.

Table 11: Huge Models: Three Trials, $\varepsilon = 0.3$, $T^{(0)} = 10$.

Model	Number of Triangles	Best Number of Tristrips	Average Computational Time	Average Macroscopic Time	Memory Usage
Asteroid300k	299,600	29,702	32 min, 56 s	147.33	139 MB
Dragon	871,414	130,106	4 h, 25 min, 50 s	235.00	390 MB

6 Conclusion

We have proposed a new heuristic method for generating sequential triangle strips for a given triangulated surface model, which represents an important hard (NP-complete) problem in computer graphics and visualization. In particular, we have reduced this stripification problem to the minimum energy problem in Hopfield networks and formally proven that there is a one-to-one correspondence between the optimal stripification representatives and the minimum energy states reachable by the Hopfield net from the initial zero state. This result is important not only from a theoretical point of view, providing an interesting relation between two combinatorial problems of different types, but the method is also practically applicable since the construction of the Hopfield net uses only a linear number of units and connections.

Thus, we have implemented the reduction in our program HTGEN (including the simulated annealing) for computing the semioptimal stripifications. We have conducted plenty of practical experiments that confirmed that HTGEN can generate smaller numbers of tristrips than those obtained by the leading conventional stripification program FTSG (a reference stripification method not based on neural nets), although the HTGEN running time grows rapidly near the global optimum. Particularly, HTGEN cannot compete with the real-time program FTSG, which provides the stripifications within a few milliseconds. Nevertheless, HTGEN can be used to generate almost optimal stripifications when one is satisfied by offline solutions at the preprocessing stage. In addition, HTGEN exhibits empirical linear time complexity for fixed parameters of simulated annealing, and the stripifications were computed using HTGEN even for huge models of hundreds of thousands of triangles in a reasonable time frame. This suggests that a rigorous approximation algorithm with a high-performance guarantee might exist for the stripification problem whose design represents an important open problem. Another challenge for future research is to generalize the method for sequential strips with zero-area triangles, which are also supported in practical graphics systems, or for nontriangular meshes.

Acknowledgments

We thank Joseph S. B. Mitchell for providing us the FTSG program for testing purposes. The presentation of this letter benefited from the valuable comments of anonymous reviewers. JŠ's research was partially supported by Information Society project 1ET100300517 and Institutional Research Plan AV0Z10300504. RL's work was partially supported by the Ministry of Education, Youth and Sports of the Czech Republic through project 1M0572.

References

Ackley, D. H., Hinton, G. E., & Sejnowski, T. J. (1985). A learning algorithm for Boltzmann machines. *Cognitive Science, 9*(1), 147–169.

Barahona, F. (1982). On the computational complexity of Ising spin glass models. *Journal of Physics A: Mathematical and General, 15*(10), 3241–3253.

Cichocki, A., & Unbehauen, R. (1993). *Neural networks for optimization and signal processing*. Chichester: Wiley.

Estkowski, R., Mitchell, J. S. B., & Xiang, X. (2002). Optimal decomposition of polygonal models into triangle strips. In *Proceedings of the 18th Annual Symposium on Computational Geometry (SCG 2002)* (pp. 254–263). New York: ACM Press.

Farhat, N. H., Psaltis, D., Prata, A., & Paek, E. (1985). Optical implementation of the Hopfield model. *Applied Optics, 24*(10), 1469–1475.

Hopfield, J. J. (1982). Neural networks and physical systems with emergent collective computational abilities. *Proceedings of the National Academy of Sciences USA, 79*, 2554–2558.

Hopfield, J. J. (1984). Neurons with graded response have collective computational properties like those of two-state neurons. *Proceedings of the National Academy of Sciences USA, 81*, 3088–3092.

Hopfield, J. J., & Tank, D. W. (1985). "Neural" computation of decisions in optimization problems. *Biological Cybernetics, 52*(3), 141–152.

Parberry, I. (1994). *Circuit complexity and neural networks.* Cambridge, MA: MIT Press.

Pospíšil, D., & Zbořil, F. (2004). Building triangle strips using Hopfield neural network. In *Proceedings of the 6th International Scientific Conference on Electronic Computers and Informatics (ECI 2004)* (pp. 394–398). Košice, Slovakia: University of Technology.

Šíma, J. (2005a). Generating sequential triangle strips by using Hopfield nets. In *Proceedings of the 7th International Conference on Adaptive and Natural Computing Algorithms (ICANNGA'2005)* (pp. 25–28). Berlin: Springer-Verlag.

Šíma, J. (2005b). Optimal triangle stripifications as minimum energy states in Hopfield nets. In *Proceedings of the 15th International Conference on Artificial Neural Networks (ICANN'2005)*, LNCS 3696 (pp. 199–204). Berlin: Springer-Verlag.

Šíma, J., & Orponen, P. (2003). General-purpose computation with neural networks: A survey of complexity theoretic results. *Neural Computation, 15*(12), 2727–2778.

Vaněček, P., & Kolingerová, I. (2007). Comparison of triangle strips algorithms. *Computers and Graphics*, *31*(1), 100–118.

Xiang, X., Held, M., & Mitchell, J. S. B. (1999). Fast and effective stripification of polygonal surface models. In *Proceedings of the ACM Symposium on Interactive 3D Graphics* (pp. 71–78). New York: ACM Press.

Received October 16, 2007; accepted June 24, 2008.